

SCIENTIFIC REPORTS



OPEN

The discovery of a novel inhibitor of apoptotic protease activating factor-1 (Apaf-1) for ischemic heart: synthesis, activity and target identification

Received: 21 August 2015

Accepted: 27 June 2016

Published: 22 July 2016

Ying Wang¹, Yang Cao², Qing Zhu³, Xianfeng Gu² & Yi Zhun Zhu^{1,4}

Apaf-1 is a central component in the apoptosis regulatory network for the treatment of apoptosis related diseases. Excessive Apaf-1 activity induced by myocardial ischemia causes cell injury. No drug targeted to Apaf-1 for treating myocardial ischemia has been reported to the best of our knowledge. In the present work, we synthesized a novel compound, ZYZ-488, which exhibited significant cardioprotective property in significantly increasing the viability of hypoxia-induced H9c2 cardiomyocytes and reducing CK and LDH leakage. Further study suggested the protective activity of ZYZ-488 dependent on its anti-apoptosis effect. This anti-apoptotic effect is most probably related to its disturbing the interaction between Apaf-1 and procaspase-9 as the target fishing and molecular docking indicated. The suppression on the activation of procaspase-9 and procaspase-3 with ZYZ-488 strongly suggested that compound ZYZ-488 could be a novel inhibitor of Apaf-1. In conclusion, ZYZ-488 as a novel small molecule competitive inhibitor of Apaf-1, with the great potential for treating cardiac ischemia.

Leonurine (LEO, also named as SCM-198) is a natural alkaloid chemically synthesized by our laboratory from *Herba leonuri* which has long been used in Chinese traditional medicine. The studies on LEO show that it has cardio^{1,2} and neuronal³ protective effects both *in vitro* and *in vivo*. The evidence in animal studies of LEO exhibits cardioprotective effects on myocardial ischemia disease in rats after oral administration. Therefore, LEO has been considered as a potential drug candidate in our laboratory for further studies. However, pharmacokinetic studies showed that the major of LEO was quickly metabolized into leonurine-10-O-β-D-glucuronide (ZYZ-488, Fig. 1) after oral administration. The level of ZYZ-488 was far higher (approximately 20-fold) than its parent drug in the pooled plasma samples after oral administration at 30 mg/kg⁴. To fully understand the mechanism of action of drugs, it is important to recognize the role of major metabolites⁵. Thus, the studies on the synthesis and the biological activity of ZYZ-488 has been further performed.

The previous studies of our group show that LEO exhibited protective effects in myocardial hypoxia, especially in anti-apoptotic assays^{1,3,6}. As we know, apoptosis is a physiological counterpart of cell replication and is the contributing cause to cardiomyocyte death during ischemia, myocardial infarction (MI) and heart failure⁷. Several reports have shown that ischemia/reperfusion-induced infarct extension can be significantly attenuated by anti-apoptotic therapy. However, apoptotic signaling networks are very intricate, regulated by a fine-tuned balance between pro-apoptotic and anti-apoptotic proteins⁸. Different cellular pathways can lead to apoptosis. For example, in the presence of ATP/dATP, the apoptosome is assembled when seven Apaf-1; cytochrome c heterodimers oligomerise to form a 'wheel' structure that has the ability to recruit procaspase-9. The cytochrome c binds the adapter molecule Apaf-1 and, it promotes the assembly of a multiprotein complex called apoptosome

¹Department of Pharmacology, School of Pharmacy, Fudan University, Shanghai 201203, China. ²Department of Medicinal Chemistry, School of Pharmacy, Fudan University, Shanghai 201203, China. ³School of Pharmacy, Nantong University, Nantong, 226001, China. ⁴School of Pharmacy, Macao University of Science and Technology, Macao. Correspondence and requests for materials should be addressed to X.G. (email: xfgu@fudan.edu.cn) or Y.Z.Z. (email: zhuyz@fudan.edu.cn or yzzhu@must.edu.mo)

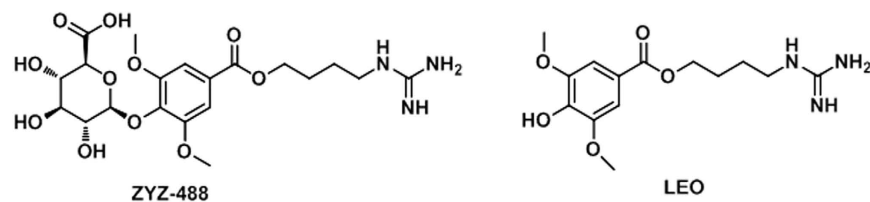


Figure 1. Chemical structures of ZYZ-488 and Leonurine.

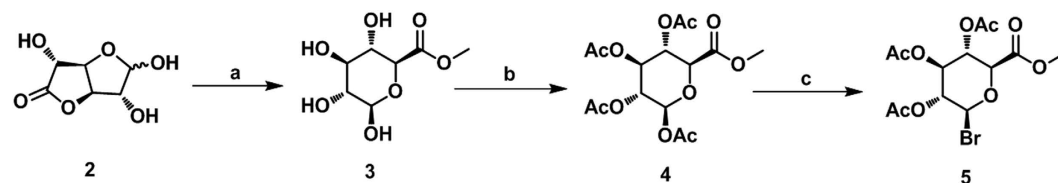


Figure 2. The synthetic route of key intermediate 5. (a) CH_3OH , NaOH , r.t., 3 h; (b) Ac_2O , HClO_4 , r.t., 12 h; (c) CH_3OH , HBr , N_2 , 0°C , 2 h.

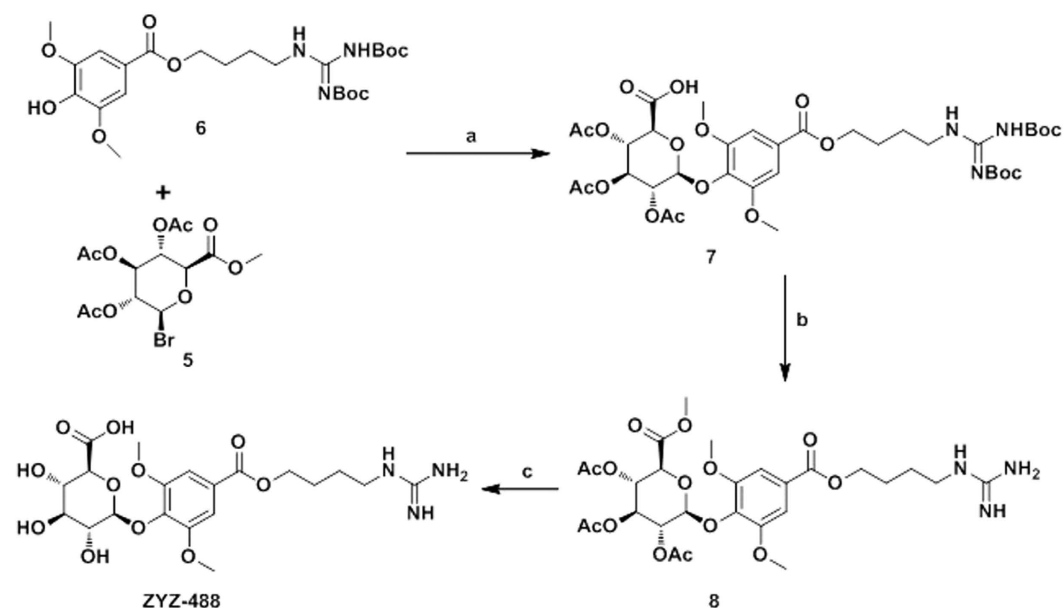


Figure 3. The synthetic route of compound ZYZ-488. (a) CHCl_3 , TBAB, K_2CO_3 , 12 h; (b) CH_2Cl_2 , TFA, r.t., 12 h; (c) $\text{CH}_2\text{Cl}_2/\text{CH}_3\text{OH}$ (1:9), guadine, 0°C , 2 h.

which, in turn, binds and activates procaspase-9, the main constituent of the apoptosome is Apaf-1, Apaf-1 is a multidomain protein with an N-terminal caspase recruitment domain (CARD), a central nucleotide-binding and oligomerization domain (NOD), and a C-terminal WD40 repeats domain⁹. Apoptosis protease-activating factor-1 (Apaf-1) has been described as a key regulator of the mitochondrial apoptosis pathway⁶ and considered an emerging pharmacological target. However, only few compounds targeting it have been tested and none of these have yet been approved by FDA for starting clinical trials. Therefore, it is imperative to develop more and new Apaf-1 inhibitors. Coincidentally, the studies on target fishing and molecular docking discovered ZYZ-488 most probably binding to Apaf-1 in procaspase-9 binding site. As expected, western blot confirmed ZYZ-488 inhibited the activation of binding protein procaspase-9, while not tampering the expression of Apaf-1, and studies on target specificity by siRNA based approaches further proved ZYZ-488 is a novel inhibitor of Apaf-1. These studies provide us a fresh insight for agent design and modification in treating ischemia.

Results

Chemistry. The synthesis of compound ZYZ-488 and key intermediate 5 is outlined in Figs 2 and 3. The preparation of key intermediate was carried out starting from glucuronic lactone (2). After treatment of NaOH

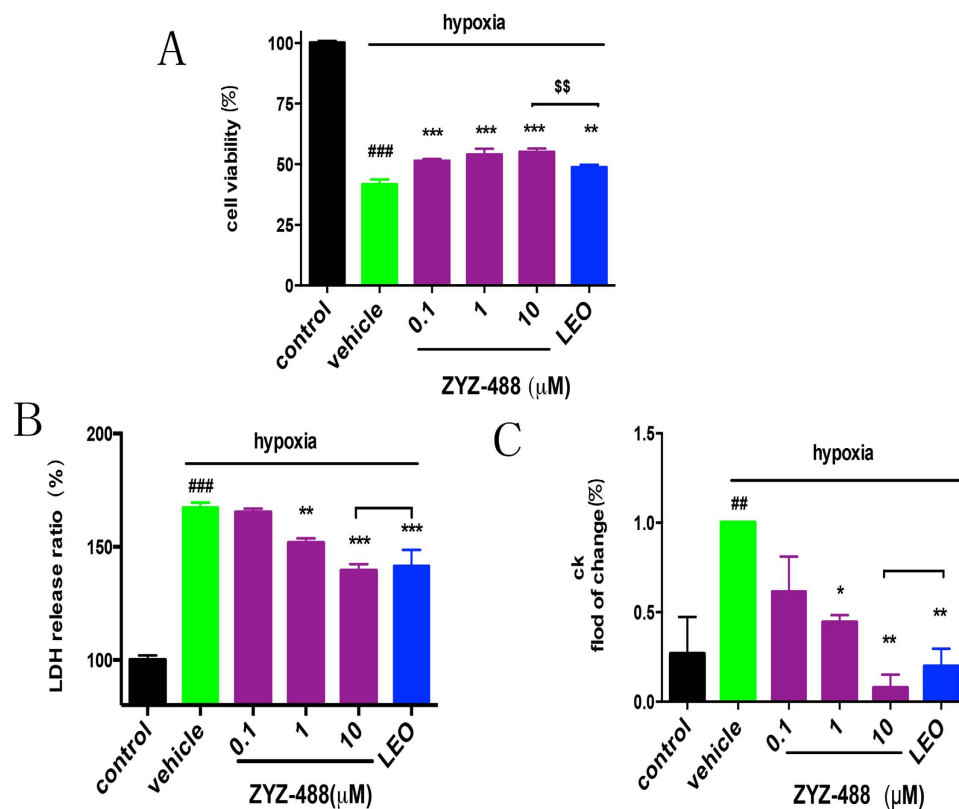


Figure 4. Analysis of the cardioprotective activities of ZYZ-488 and LEO (10 μM) in hypoxia-induced H9c2 rat ventricular cells. (A) Effects of different dosed ZYZ-488 and LEO on cell viability in hypoxia-induced H9c2 rat ventricular cells. (B) Effects of ZYZ-488, LEO on LDH leakage in hypoxia-induced H9c2 rat ventricular cells. (C) Effects of ZYZ-488, LEO on CK activity in hypoxia-induced H9c2 rat ventricular cells. H9c2 cells were treated with ZYZ-488, LEO in hypoxia for 12 h. $^{\#}P < 0.05$; $^{\#\#}P < 0.01$; $^{\#\#\#}P < 0.001$ versus control group. $^*P < 0.05$; $^{**}P < 0.01$; $^{***}P < 0.001$ versus vehicle group. $^{SS}P < 0.01$ versus LEO 10 μM treatment group. Error bars represent the data obtained from the experiments repeated three times or more.

and methanol, the resulting methyl ester **3** was acetylated by Ac_2O and HClO_4 to afford the intermediate **4**. Subsequently, **4** was treated with HBr in acetic acid to give desired intermediate **5**.

To prepare target compound ZYZ-488, intermediate **5** condensed with another key intermediate **6** which was prepared as previously described¹⁰, to afford **7**. Finally, the Boc groups in compound **7** were removed by trifluoroacetic acid (TFA) followed by hydrolyzation by guanidine to give target compound ZYZ-488.

Protective effects of compound ZYZ-488 on hypoxia-induced H9c2 rat ventricular cells. The synthetic ZYZ-488 and LEO were evaluated on their protective effects against hypoxia in H9c2 rat ventricular cells. The effects of compound ZYZ-488, and LEO were investigated by cell counting kit-8 (CCK8) assay which demonstrates cell viability. It showed that the hypoxic condition had an effect on H9c2 rat ventricular viability compared with the normoxic control group ($P < 0.001$). Cells were treated with 0.1, 1, and 10 μM of ZYZ-488 and 10 μM of LEO during hypoxia for 12 hours. Treatment of ZYZ-488 led to increase in the number of surviving cells at a concentration-dependent manner [0.1 μM ($51.46 \pm 7.42\%$), 1 μM ($54.15 \pm 2.26\%$), 10 μM ($55.19 \pm 1.28\%$)] compared to vehicle group (41.76 ± 1.90). Most interestingly, 10 μM of compound ZYZ-488 showed stronger activity on promoting the cell vitality compared with the group treated by LEO in same concentration ($P < 0.01$) (Fig. 4A). Lactic dehydrogenase (LDH) leakage (percentage of normoxic control group) into the culture medium after the induction of hypoxia was significantly higher than that in the normoxic control group [($167.37 \pm 2.20\%$) vs (100%)]. Compared with the vehicle group, 1 μM and 10 μM of compound ZYZ-488 and 10 μM of LEO remarkably inhibited LDH leakage into medium which is the marker of cell membrane integrity¹¹ ($P < 0.05$) (Fig. 4B). Elevated Creatine Kinase (CK) is a canonical index of myocardial infarction in clinical diagnosis. Hypoxia caused cell injury, thus resulting in increased CK leakage into the culture medium¹² than the normoxic group [(100%) vs ($26.8 \pm 20.64\%$)]. In our experiment, CK leakage was significantly reduced when cardiomyocytes were treated with ZYZ-488 at 1 μM [($44.49 \pm 3.92\%$)] and 10 μM [($7.848 \pm 7.39\%$)] and LEO at 10 μM [($19.75 \pm 9.93\%$)] (Fig. 4C), suggesting that ZYZ-488 was more potent than LEO in increasing cell viability against hypoxia ($P < 0.01$). Thus, the results above confirmed that ZYZ-488 exhibited significant, even more potent cardioprotective activity than LEO in hypoxia-induced H9c2 cells injury.

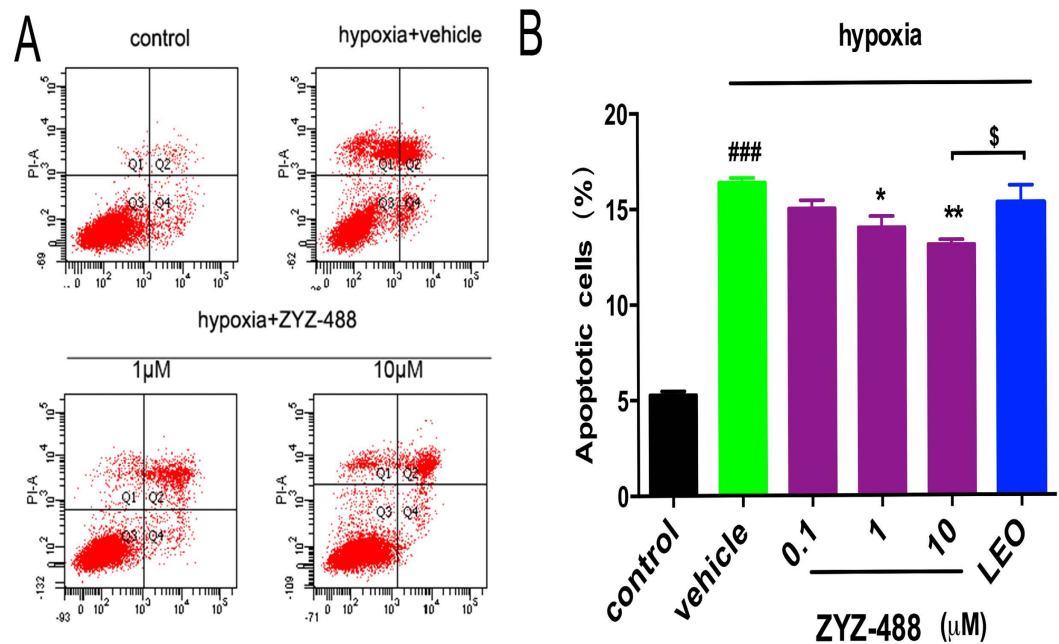


Figure 5. (A) Apoptosis fraction of hypoxia-induced H9c2 rat ventricular cells with or without **ZYZ-488** and **LEO** was measured by Annexin V-FITC/PI assay. (B) Percentage of apoptotic cardiomyocytes under the treatment of **ZYZ-488** and **LEO** was then analyzed based on Annexin V-FITC/PI stain. $###P < 0.001$ versus control group. $*P < 0.05$; $**P < 0.01$; $***P < 0.001$ versus vehicle group. $^{\$}P < 0.01$ versus **LEO** 10 μM treatment group.

Compound ZYZ-488 decreased apoptosis in hypoxic H9c2 cells. Apoptosis is responsible for a significant amount of the cardiomyocyte death that contributes to the development and progression of heart failure¹³. It has been shown that hypoxia represents the most physiologically relevant stresses lead to rapid apoptosis^{14–16}. The apoptotic cell counts were measured using Annexin V-FITC/PI by flow cytometry. The results displayed that **ZYZ-488** and **LEO** decreased the number of apoptotic cells (Fig. 5A). The percentage of cells showing an apoptotic pattern (including early apoptotic and late apoptotic cells) was significantly decreased with **ZYZ-488** at 1 μM [(14.00 \pm 0.59)%], 10 μM [(13.1 \pm 0.26)%] and **LEO** at 10 μM [(15.28 \pm 0.92)%] compared with vehicle group [(16.38 \pm 0.13)%] (Fig. 5B). Imaging of treated cells was done using a confocal microscope. Marked cellular morphological characteristics of apoptosis, such as condensation of chromatin and nuclear fragmentation, were clearly seen using Hoechst 33258 staining (Fig. 6). As demonstrated above, **ZYZ-488** is potent in protecting myocardial cells from hypoxia injury. According to the anti-apoptotic results, we speculate **ZYZ-488** elicits cardioprotective effects through its anti-apoptotic activity.

Prediction of molecular target of compound ZYZ-488. Cell apoptosis involves complex signaling network. To identify potential targeting candidates of compound **ZYZ-488**, *in-silico* targets screening was conducted. PharmMapper server, a reverse pharmacophore mapping approach was performed using an in-house pharmacophore database (PharmTargetDB)¹⁷. Apoptotic protease-activating factor 1 (Apaf-1), a key regulator of the apoptosis machinery¹⁸, is in the top 0.3% of prediction results. Combining with our results of anti-apoptotic activity of **ZYZ-488**, we speculated that compound **ZYZ-488** might interact with Apaf-1 to suppress the apoptosis, then elicit the protective effect on H9c2 cells. It has been established that binding of caspase recruitment domain (CARD) of Apaf-1 to procaspase-9 leads to apoptotic cell death¹⁹. X-ray crystal structure of the complex of Apaf-1 CARD binding with the procaspase-9 prodomain (PDB code: 3YGS) has been determined at 2.5 Å resolution by Shi *et al.*²⁰. Three arginine residues (Arg 13, Arg 52, and Arg 56) from procaspase-9 prodomain were identified to play a vital role in the stability of the Apaf-1 CARD/procaspase-9 prodomain complex. Hydrogen bonds network could be observed between these three arginine residues and Asp 27/Glu 40 from Apaf-1 CARD²⁰. In view of the common basic guanidyl groups, leonurine and **ZYZ-488** may be capable of binding to the acidic residues of Apaf-1 CARD as mimics of Arg 13/Arg 52/Arg 56 in procaspase-9 prodomain. Interestingly, this presumption was perfectly supported by molecular docking studies on leonurine or **ZYZ-488**/Apaf-1 CARD complex using Schrodinger software suite 2015. As depicted in Fig. 7A, in the binding mode predicted by docking, the electropositive guanidyl group of leonurine forms four hydrogen bonds (2.1 Å, 2.1 Å, 2.0 Å, 1.6 Å) with the electronegative side chains of Asp 27 and Glu 40. The hydrogen bonds network is of great importance in the binding of the Apaf-1 CARD/procaspase-9 prodomain complex¹⁸. In addition, the 3-OH of leonurine could accept two hydrogen bonds (2.4 Å, 1.9 Å) from the side chain of Arg 44 in Apaf-1 CARD. As in the case of **ZYZ-488**/Apaf-1 CARD (Fig. 7B), more favorable interactions could be found. Similarly, four hydrogen bonds (2.3 Å, 2.2 Å, 2.1 Å, 1.7 Å) between the guanidyl group of **ZYZ-488** and the two acidic residues of Apaf-1 CARD (Asp 27 and Glu 40) could be observed. Apart from that, **ZYZ-488** anchors the glucuronic acid moiety in a positive center formed by

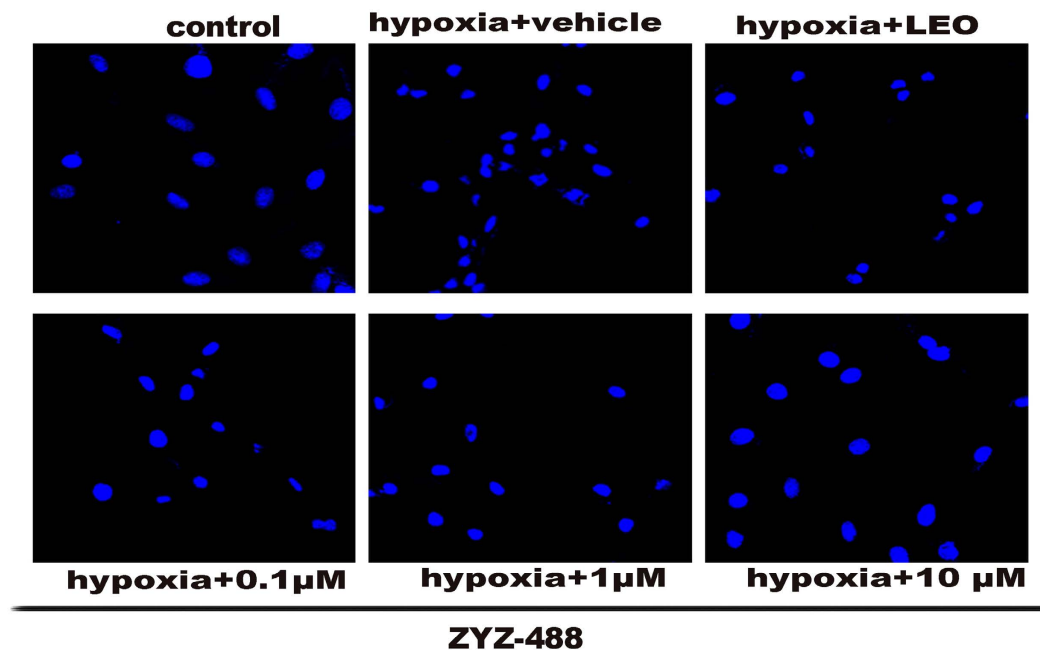


Figure 6. Hoechst staining H9c2 cells exposed to normoxia or hypoxia for 12 h in the absence or presence of ZYZ-488 and LEO, H9c2 cells apoptosis were observed by confocal microscopy.

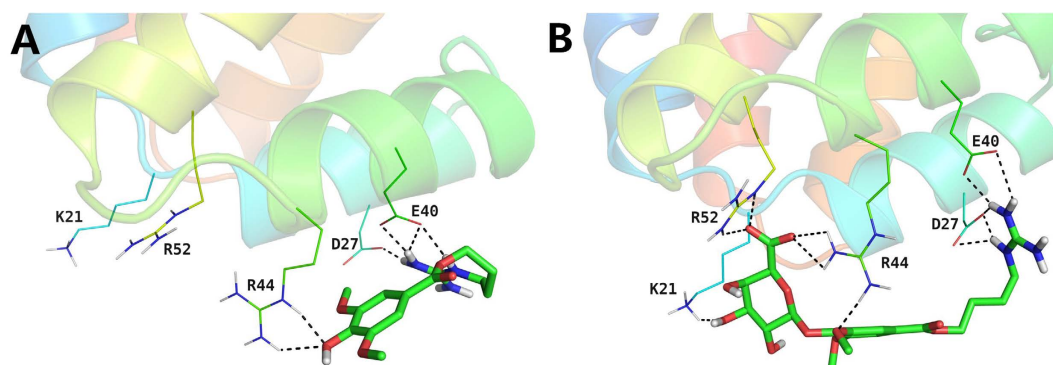


Figure 7. Overlapped poses of LEO (A) and compound ZYZ-488 (B) at the procaspase-9 binding site of Apaf-1. The ligands are shown in sticks. The coloring for oxygen atoms of each compound is red. The hydrogen bonds are denoted with dashed lines. Structure figures were prepared using LigPrep (Schrödinger Release 2015-4: LigPrep, version 3.6, Schrödinger, LLC, New York, NY, 2015).

Lys 21, Arg 44, and Arg 52 of Apaf-1 CARD. Hence, the binding of ZYZ-488 are more stable. These results indicate that leonurine and ZYZ-488 could occupy the caspase recruitment site of Apaf-1, thus block its interaction with procaspase-9, further resulting in the observed anti-apoptotic effect *in vitro*. Moreover, the more significant anti-apoptotic effect of ZYZ-488 as compared with leonurine may be attributed to the additional interactions of the glucuronic acid moiety binding to the positive center in Apaf-1 CARD.

Identification of Molecular target of compound ZYZ-488. Apaf-1 plays a critical role in apoptosis by binding to and activating procaspase-9. Activation of procaspase-9 initiates a protease cascade that subsequently activates downstream procaspase-3, leading to the cleavage of target proteins and then orderly demise of the cell²¹. Based on the interaction between ZYZ-488 and Apaf-1 described as above, we infer that ZYZ-488 could bind to Apaf-1 at the Apaf-1/procaspase-9 binding site, antagonizing the activation of procaspase-9. To validate this deduction, the effect of compound ZYZ-488 on the Apaf-1's activation of procaspase-9 and downstream signaling pathways were determined in H9c2 cells by western blot analysis. The results showed that hypoxia promoted activation of procaspase-9 compared with control group, this activation were remarkably inhibited in a dose-dependent manner after the treatment of compound ZYZ-488 (Fig. 8 and Fig. S10). Consistently, the downstream procaspase-3's activation were obviously declined with the exposure to compound ZYZ-488.

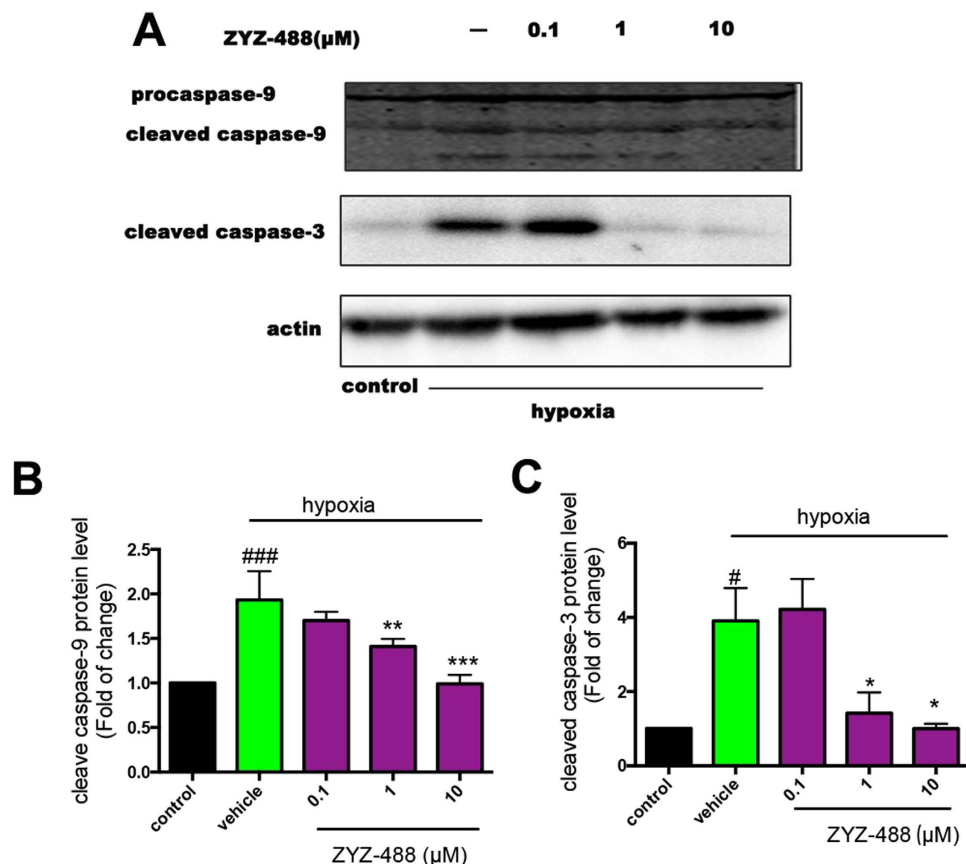


Figure 8. Effects of compound ZYZ-488 on activation of caspase-9 and caspase-3. H9c2 cells were exposed to normoxia or hypoxia for 12 h with or without ZYZ-488 treatment. (A) Representative Western blot showed hypoxia induced Apaf-1-mediated activation of procaspase-9 and procaspase-3 was inhibited by ZYZ-488. Bar graphs represent the quantitative difference in protein level of caspase-9 (B) and caspase-3 (C). $###P < 0.001$, $*P < 0.05$ versus control group. $*P < 0.05$; $**P < 0.01$; $***P < 0.001$ versus vehicle group. Data are the mean \pm S.E.M of results from at least three independent experiments.

To exclude the possibility that ZYZ-488 exerts its inhibitory effects through down regulation of Apaf-1 expression, we examined Apaf-1 expression after ZYZ-488 treatment in normoxic and hypoxic condition (Figs S7 and S12). As shown in Fig. S7, compound ZYZ-488 did not affect the expression of Apaf-1 compared with vehicle group.

The protective effect of ZYZ-488 requires the presence of Apaf-1 in H9c2 cells. In order to explore if all the observed effects were dependent on the direct Apaf-1 inhibition, the studies on target specificity was performed in cellular models by siRNA based approaches. The silencing effect towards Apaf-1 was observed with three different siRNA (Fig. S9). The siRNA79389 was selected for the silence of Apaf-1. The apoptotic cell counts were significantly increased in hypoxia condition [(16.73 \pm 3.02)%] compared with control group [(5.93 \pm 0.25)%] (Fig. 9A,B). However, we discovered that hypoxia-induced cell apoptosis can't be inhibited by ZYZ-488 in Apaf-1 siRNA-based knock down H9c2 cells. As showed in Fig. 9B that the apoptotic H9c2 cells induced by hypoxia with ZYZ-488 treatment [(18.77 \pm 1.11)%] display no significant change with vehicle group [(17.70 \pm 2.56)%]. Results present the inhibition of apoptosis is lost when Apaf-1 is silenced. These results correlated with the western blot of caspase-9 (Fig. 9C and Fig. S11), suggesting that the inhibitory towards caspase-9 activation of ZYZ-488 dependent on the levels of Apaf-1 in the cell. Taken together, we propose that ZYZ-488 could competitively bind to Apaf-1 against procaspase-9, and thus tampering the activation of procaspase-9.

Discussion

Apaf-1 is a rather large protein (130kDa) that carries multiple functional domains, namely an N-terminal caspase activation recruitment domain (CARD), the CED4 homology domain (which include the dATP/ATP-binding motif), as well as 13 C-terminal WD-40 repeats, which allow for its interaction with Cyt c and for its oligomerization. Apaf-1 is the molecular core of the apoptosome, a multiproteic complex mediating the so-called mitochondrial pathway of cell death²². However, there is few reports on Apaf-1 pharmacological inhibition. Nelson Chau²³ reported Aven an endogenous protein has the ability to complex with Apaf-1 and inhibit self-association of Apaf-1 raises the possibility that Aven may impair oligomerization of Apaf-1. Malet²⁴ *et al.* identified a novel class of trialkylglycine-based molecules that binds reversibly to Apaf-1 in a cytochrome *c* noncompetitive manner and precludes the recruitment and activation of procaspase-9. QM31²⁵ was reported as a chemical inhibitor of

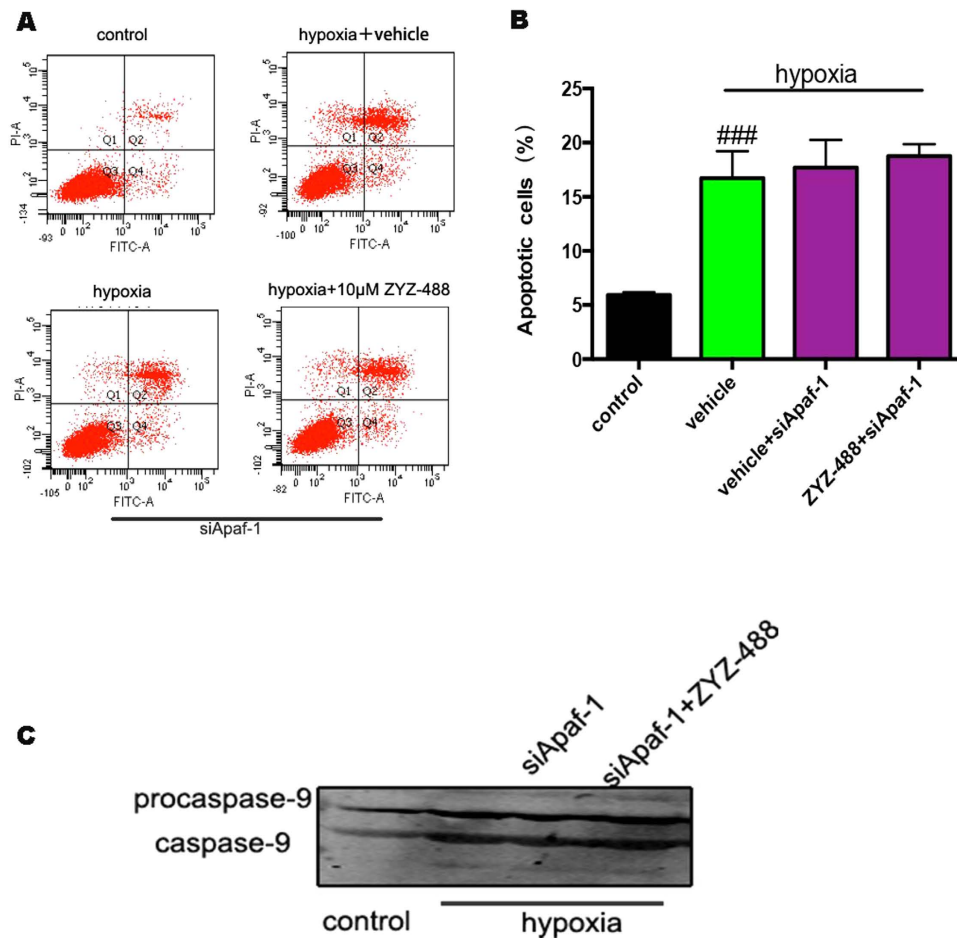


Figure 9. Apaf-1 is required for the inhibitory activity of ZYZ-488. Apaf-1 was silenced in H9c2 cells by Apaf-1 siRNA. (A) Apoptosis fraction of hypoxia-induced H9c2 cells were measured in presence or absence of ZYZ-488 treatment. (B) Percentage of apoptotic cardiomyocytes were analyzed. $###P < 0.001$ versus control group. Data are the mean \pm S.E.M of results from at least three independent experiments. (C) Representative Western blot showed caspase-9 activity for control or Apaf-1 (siApaf-1) silencing in the presence or absence of ZYZ-488 treatment.

Apaf-1 exerts mitochondria-protective functions while the direct interaction between QM31 and Apaf-1 was not clearly defined. Mar⁹ *et al.* demonstrated SVT016426 avoid apoptosis, and the effects were dependent on Apaf-1 inhibition through the lost of effect in siRNA knockdown cells. They proposed that the SVT family of Apaf-1 inhibitors binds to Apaf-1 at the CARD-NOD interface or at the reported dATP binding site in the NOD domain.

Here, we have successfully synthesized an active metabolite of LEO, compound ZYZ-488. Pharmacological evaluation showed ZYZ-488 possessed potent cardioprotective effects, which was elicited through its suppression of hypoxia-induced apoptosis. It is important to note that ZYZ-488 has stronger anti-apoptotic effects than its parent drug LEO. Different from the inhibitors mentioned above, molecular docking results suggest the similarity between ZYZ-488 and the arginine of procaspase-9 prodomain makes ZYZ-488 capable of inhibiting Apaf-1 recruitment and activation of procaspase-9 as a mimic of procaspase-9 which could competitively bind to Apaf-1 against procaspase-9, and thus tampering the activation of proprocaspase-9 and procaspase-3. Most importantly, compound ZYZ-488 did not show any noticeable effect in H9c2 cells where Apaf-1 was knocked down, which demonstrate the anti-apoptotic effect of ZYZ-488 indeed dependent on Apaf-1 inhibition. In summary, we propose compound ZYZ-488 as a novel competitive, synthetic small molecule inhibitor of Apaf-1 acting through interaction with Apaf-1 in procaspase-9 binding site.

Methods

General. All chemical reagents and solvents were purchased from commercial sources and used without further purification. Thin-layer chromatography (TLC) was performed on silica gel plates. Column chromatography were performed using silica gel (Hailang, Qingdao), 200–300 mesh and MCI gel CHP20P (Mitsubishi chemical, Japan). NMR spectra were recorded employing a 400 or 600 MHz Bruker spectrometer. Mass spectral data was collected on a HP5973 N analytical mass spectrometer. HRMS data were determined on an IonSpec 4.7 T FTMS instrument. All reagents of cell culture were purchased from Sigma (St. Louis, MO) unless otherwise stated. The following substances Dulbecco's Modified Eagle medium (DMEM) and calf serum were purchased from Invitrogen Inc. (MD, USA). All antibodies used for western blotting in this study were from Cell Signaling

Technology, Inc. (MA, US). The kits for, Lactic Dehydrogenase (LDH), Creatine Kinase (CK), were obtained from Jiancheng Bioengineering Institute (Nanjing, China). The kit for cell counting kit-8, Hoechst staining was obtained from Beyotime Bioengineering Institute (Lianyungang, China). AnnexinV-FITC/PI kit were obtained from Becton, Dickinson and Company (USA).

The purities of all newly synthesized compounds were analyzed by HPLC, with over 95% of purity. Analytical HPLC was performed on a Waters 600E system chromatograph equipped with photodiode array detector using a MG-C18 5 μ m 250 mm 4.6 mm column (reverse phase) to detect the purity of the products. The mobile phase was a gradient of 30% methanol flow rate of 1.0 mL/min.

(2S,3R,4S,5S,6S)-2-(4-((Z)-8-((tert-butoxycarbonyl)amino)-12,12-dimethyl-10-oxo-2,11-dioxo-7,9-diazatridec-8-en-1-oyl)-2,6-dimethoxyphenoxy)-6-(methoxycarbonyl)tetrahydro-2H-pyran-3,4,5-triyl triacetate (7). Bromo-sugar **5** (27.6 g, 0.0693 mol) and **6** (35.4 g, 0.0693 mol) was dissolved in CHCl_3 (25 mL). To the above stirred solution Tetrabutyl ammonium bromide (22.4 g, 0.0693 mol) and K_2CO_3 (0.2 mol/L, 26 mL) were added. The reaction mixture was heated at 45 °C for 12 h. After completion of the reaction, CHCl_3 (25 mL) was added, and then washed by 1N HCl, saturated NaHCO_3 (2 \times 25 mL) and brine (2 \times 25 mL). The organic layer was separated, dried over Na_2SO_4 , the solvent was evaporated. The residue was purified by column chromatography on silica gel to afford compound **7** 11.2 g (40% yield). ^1H NMR (400 MHz, CDCl_3): δ 6.93 (s, 2H), 5.60 (t, 1H, $J = 7.44$ Hz), 5.47–5.21 (m, 3H), 4.34 (t, 2H, $J = 6.3$ Hz), 4.12 (q, 1H, $J = 8$ Hz), 3.88 (s, 6H), 3.68 (s, 3H), 3.52 (dd, 2H, $J_1 = 8$ Hz, $J_2 = 12$ Hz), 2.05 (s, 9H), 1.83 (m, 2H), 1.74 (m, 2H), 1.49 (s, 9H), 1.48 (s, 9H). ^{13}C NMR (400 MHz, CDCl_3): δ 170.24, 169.40, 169.19, 167.08, 165.93, 155.99, 153.25, 152.73, 152.73, 137.84, 126.67, 106.93, 100.33, 83.47, 79.88, 77.39, 77.07, 76.75, 72.75, 72.40, 71.86, 56.43, 52.69, 40.65, 28.21, 26.15, 25.82, 20.65. HRMS (ESI): calculated for $\text{C}_{37}\text{H}_{53}\text{N}_3\text{O}_{18}$ $[\text{M} + \text{H}]^+$ 828.3397, found 828.3404.

(2S,3R,4S,5S,6S)-2-(4-((4-guanidinobutoxy)carbonyl)-2,6-dimethoxyphenoxy)-6-(methoxycarbonyl)tetrahydro-2H-pyran-3,4,5-triyl triacetate (8). Compound **7** (1.2 g, 1.45 mmol) was dissolved in 10 mL CH_2Cl_2 :TFA (1:1, v/v) solution and stirred for 12 h. Saturated NaHCO_3 solution (100 mL) was added to the reaction mixture and stirred for 30 min. Then extracted with CH_2Cl_2 , The organic layer was separated, dried over Na_2SO_4 , the solvent was evaporated to provide yellow solid compound **8** (yield 92%) ^1H NMR (400 MHz, D_2O): δ 7.20 (s, 2H), 5.47–5.21 (m, 3H), 5.04 (d, 1H, $J = 6.7$ Hz), 4.34 (d, 2H, $J = 4.9$ Hz), 3.71 (s, 6H), 3.68 (s, 3H), 3.25–.01 (m, 4H), 2.75 (t, 2H, $J = 6$ Hz), 2.05 (s, 9H), 1.61 (dt, 4H, $J_1 = 32$ Hz, $J_2 = 4$ Hz), ^{13}C NMR (150 MHz, CDOD_3): δ 173.75, 172.83, 168.44, 168.37, 159.64, 149.93, 141.04, 128.57, 109.40, 105.29, 103.73, 78.4, 78.11, 76.31, 74.06, 66.03, 58.06, 58.00, 57.84, 43.04, 27.96, 27.56 24.48, 22.03. HRMS (ESI): calculated for $\text{C}_{27}\text{H}_{37}\text{N}_3\text{O}_{14}$ $[\text{M} + \text{H}]^+$ 628.2348, found 628.2357.

(2S,3S,4S,5R,6R)-6-(4-((4-guanidinobutoxy)carbonyl)-2,6-dihydroxyphenoxy)-3,4,5-trihydroxytetrahydro-2H-pyran-2-carboxylic acid (ZYZ-488). Compound **8** (6.27 g, 10 mmol) was dissolved in 50 mL CH_2Cl_2 :MeOH (1:9, v/v) solution and cooled to 0 °C, and then fresh guanine in ethanol was added and stirred for 2 h, immediately there was yellow solid deposited. The solid was filtrated and then purified by column chromatography on MCI CHP20 gel to provide **ZYZ-488** (508 mg, yield 11%). ^1H NMR (600 MHz, D_2O): δ 6.93 (s, 2H), 5.04 (d, 1H, $J = 11.6$ Hz), 4.04 (d, 2H, $J = 6.9$ Hz), 3.71 (s, 6H), 3.59–3.47 (m, 4H), 3.09 (t, 2H, $J = 6.43$ Hz), 1.61 (dt, 4H, $J_1 = 5.6$ Hz, $J_2 = 13$ Hz). ^{13}C NMR (150 MHz, C): δ 175.24, 167.11, 156.65, 151.93, 137.51, 125.69, 106.66, 102.29, 77.12, 75.47, 73.56, 71.80, 65.43, 56.05, 40.67, 25.01, 24.66. HRMS (ESI) calculated for $\text{C}_{20}\text{H}_{29}\text{N}_3\text{O}_{11}$ $[\text{M} + \text{H}]^+$ 488.1875, found 488.187

Cell lines and induction of hypoxia. H9c2 rat ventricular cardiomyocytes (ATCC, Manassas, VA) were cultured in Dulbecco's modified Eagle medium (Gibco-Invitrogen, Carlsbad, CA) supplemented with 10% fetal bovine serum, in tissue culture flasks at 37 °C in a humidified atmosphere of 5% CO_2 . The cells were fed every 2–3 days and subcultured once they reached 70%–80% confluence. Hypoxia was induced based on the technique described by Rakhit *et al.*²⁶. All culture plates, excluding the normoxic control, were placed in an ischemia solution (composition (in mmol/L): NaCl 116; KCl 50; CaCl_2 1.8; $\text{MgCl}_2 \cdot 6\text{H}_2\text{O}$ 2; NaHCO_3 26; $\text{NaH}_2\text{PO}_4 \cdot 2\text{H}_2\text{O}$ 1) in an anaerobic chamber (BD Diagnostics System, Maryland, NJ, USA) maintained at 37 °C with a humidified atmosphere of 5% CO_2 , 10% H_2 and 85% N_2 . Chambers were sealed before incubation at 37 °C for 5 h. Normoxic incubation of myocytes in serum-free DMEM was conducted in a water-jacked incubator gassed with 95% air and 5% CO_2 at 37 °C for the same length of time. LipofectamineTM 2000 (Invitrogen) was used according to the manufacturer's instructions to transfect H9c2 cells and Apaf-1 siRNA (GenePharma, Shanghai).

Cell Survival Assay. The effects of **ZYZ-488** and **LEO** on cardiomyocyte viability were obtained using cell counting kit-8 (CCK8) assay. Briefly, H9c2 cells were seeded on 96-well plates (approximately 8000 cells/well) in Dulbecco's modified Eagle medium culture medium and maintained in regular growth medium for 2 days. The culture medium was then changed to ischemia solution with or without drugs, placed in an anaerobic chamber for hypoxia induction, then incubated at 37 °C for 12 h. After adding 10 μ L of the CCK-8 reagent to each well, the wells were incubated for 1 h at 37 °C and 5% CO_2 . The absorbance of each well were measured at 450 nm in a microtiter plate reader.

Determination of Lactate Dehydrogenase in Culture Medium. Creatine Kinase leakage into the culture medium was analyzed using Creatine Kinase Kit (Biotime, Haimen, China). CK release was expressed as a fold relative to the activity in normoxic cells.

Assessment of Apoptosis by Flow Cytometry. Apoptosis and necrosis were identified by means of double fluorescence staining with annexin V-propidium iodide. Cardiomyocytes (1×10^5 cells per sample) were

loaded with 5 μ L PI and 10 μ L Annexin V-FITC (BD,USA) at room temperature for 15 minutes in the dark. Flow cytometric analysis was performed using a flow cytometer (Becton- Dickinson, Mountain View, CA), after of Annexin-PI labeling.

Fluorescent staining of nuclei. H9c2 nuclei were stained with chromatin dye (Hoechst 33258). Briefly, cells were fixed with 3.7% paraformaldehyde for 10 minutes at room temperature, washed twice with phosphate buffered solution (PBS), and incubated with 10 μ M hoechst 33258 in PBS at room temperature for 30 min. After three washes, cells were observed under a confocal microscope (LSM 510, ZEISS).

Molecular Simulation and Physicochemical Properties calculationh. Docking studies were carried out using Schrodinger modeling suite¹⁹. The X-ray crystallographic structure of Apaf-1¹⁸ (PDB code: 1CY5) was taken from Protein Data Bank. Crystal water molecules were deleted. All missing hydrogen atoms were added by standard protein preparation protocol within Maestro followed by energy minimization using OPLS 2005 force field to optimize all hydrogen bonding networks. The structures of leonurine and ZYZ-488 were prepared with the default pK_a range of 7.0 \pm 2.0 in the ligand preparation program LigPrep²⁷. Docking of both compounds were carried out using Glide²⁸ with standard precision protocol (Small-Molecule Drug Discovery Suite 2015-4: Glide, version 6.9, Schrödinger, LLC, New York, NY, 2015). The vander Waals radii of nonpolar atoms for each of the ligands were scaled by a factor of 0.8 to account for structure variability to specific ligand binding.

Western blot analysis. Cultured H9c2 cells were harvested by scraping and centrifugation, washed with PBS, and re-suspended in RIPA buffer. Soluble proteins were collected by centrifugation at 12,000 g. Protein lysates were subjected to 10% and 12% SDS-PAGE and transferred onto a NC membrane (Millipore Corporation). After blocking with 5% skim milk, the membranes were incubated with the respective primary antibodies (caspase-3, 1:1000; caspase-9, 1:1000, Apaf-1, 1:1000 Cell Signaling Technology, USA) in Tris-buffered saline (TBS) containing 0.1% Tween-20 overnight at 4 °C. The membranes were then incubated with the appropriate secondary horseradish peroxidase-conjugated IgG antibodies at a 1:5000 dilution (Proteintech Group Inc., USA). Immunoreactive proteins were then visualized using ECL. The signals were quantified by densitometry using a Western blotting detection system (Bio-Rad Laboratories, Inc, USA). Actin served as the loading control.

Statistical analysis. Values are shown as means \pm S.E.M of at least 3 independent preparations. The significance of differences between groups was evaluated with t tests or one-way ANOVA followed by the Dunnett's multiple comparison tests. Values of P < 0.05 were considered significant. All statistics were carried out using PRISM 6.0 for MAC.

References

- Xin, H., Liu, X. H. & Zhu, Y. Z. Herba leonurine attenuates doxorubicin-induced apoptosis in H9c2 cardiac muscle cells. *Eur. J Pharmacol.* **612**, 75–79 (2009).
- Liu, X.-H. *et al.* Leonurine (SCM-198) attenuates myocardial fibrotic response via inhibition of NADPH oxidase 4. *Free Radical Biol. Med.* **54**, 93–104 (2013).
- Loh, K. P. *et al.* Leonurine protects middle cerebral artery occluded rats through antioxidant effect and regulation of mitochondrial function. *Stroke* **41**, 2661–2668 (2010).
- Zhu, Q. *et al.* Characterization of metabolites of leonurine (SCM-198) in rats after oral administration by liquid chromatography/tandem mass spectrometry and NMR spectrometry. *Scient. World J.* **2014**, 947946 (2014).
- Fura, A. Role of pharmacologically active metabolites in drug discovery and development. *Drug Discov. Today* **11**, 133–142 (2006).
- Liu, X., Pan, L., Chen, P. & Zhu, Y. Leonurine improves ischemia-induced myocardial injury through antioxidative activity. *Phytomed.* **17**, 753–759 (2010).
- Campioni, M. *et al.* Role of Apaf-1, a key regulator of apoptosis, in melanoma progression and chemoresistance. *Exp. dermatol.* **14**, 811–818 (2005).
- Lavrik, I. N. Systems biology of apoptosis signaling networks. *Curr. opin. biotech.* **21**, 551–555 (2010).
- Orzaez, M. *et al.* Apaf-1 inhibitors protect from unwanted cell death in *in vivo* models of kidney ischemia and chemotherapy induced ototoxicity. *PLoS one* **9**, e110979 (2014).
- Iddon, L., Bragg, R. A., Harding, J. R. & Stachulski, A. V. A convenient new synthesis of quaternary ammonium glucuronides of drug molecules. *Tetrahedron* **66**, 537–541 (2010).
- Liu, C. *et al.* Leonurine-cysteine analog conjugates as a new class of multifunctional anti-myocardial ischemia agent. *Eur. J Med. Chem.* **46**, 3996–4009 (2011).
- Liu, C., Gu, X. & Zhu, Y. Z. Synthesis and biological evaluation of novel leonurine-SPRC conjugate as cardioprotective agents. *Bioorg. Med. Chem. Letts* **20**, 6942–6946 (2010).
- Takemura, G., Kanoh, M., Minatoguchi, S. & Fujiwara, H. Cardiomyocyte apoptosis in the failing heart—a critical review from definition and classification of cell death. *Int. J. Cardiol.* **167**, 2373–2386 (2013).
- Liu, X., Pan, L., Gong, Q. & Zhu, Y. Leonurine (SCM-198) improves cardiac recovery in rat during chronic infarction. *Eur. J Pharmacol.* **649**, 236–241 (2010).
- Kajstura, J. *et al.* Apoptotic and necrotic myocyte cell deaths are independent contributing variables of infarct size in rats. *Lab. invest.* **74**, 86–107 (1996).
- Dogliotti, G. *et al.* Okadaic acid induces apoptosis in Down syndrome fibroblasts. *Toxicol. in Vitro: an international journal published in association with BIBRA* **24**, 815–821 (2010).
- Chen, Z. *et al.* Acenaphtho[1,2-b]pyrrole-based selective fibroblast growth factor receptors 1 (FGFR1) inhibitors: design, synthesis, and biological activity. *J. Med. Chem.* **54**, 3732–3745 (2011).
- Nicholls, A., Sharp, K. A. & Honig, B. Protein folding and association: insights from the interfacial and thermodynamic properties of hydrocarbons. *Proteins: Structure, Function, and Bioinformatics* **11**, 281–296 (1991).
- Vaughn, D. E., Rodriguez, J., Lazebnik, Y. & Joshua-Tor, L. Crystal structure of Apaf-1 caspase recruitment domain: an α -helical Greek key fold for apoptotic signaling. *J. Molecul. biol.* **293**, 439–447 (1999).
- Qin, H. *et al.* Structural basis of procaspase-9 recruitment by the apoptotic protease-activating factor 1. *Nature* **399**, 549–557 (1999).
- Hu, Y., Benedict, M. A., Ding, L. & Núñez, G. Role of cytochrome c and dATP/ATP hydrolysis in Apaf-1 mediated caspase-9 activation and apoptosis. *EMBO J.* **18**, 3586–3595 (1999).
- Ferraro, E., Corvaro, M. & Cecconi, F. Physiological and pathological roles of Apaf1 and the apoptosome. *J. Cellul. Molecul. Med.* **7**, 21–34 (2003).

23. Chau, B. N., Cheng, E. H.-Y., Kerr, D. A. & Hardwick, J. M. Aven, a novel inhibitor of caspase activation, binds Bcl-x L and Apaf-1. *Molecul. Cell* **6**, 31–40 (2000).
24. Malet, G. *et al.* Small molecule inhibitors of Apaf-1-related caspase- 3/-9 activation that control mitochondrial-dependent apoptosis. *Cell Death and Differ.* **13**, 1523–1532 (2006).
25. Mondragon, L. *et al.* A chemical inhibitor of Apaf-1 exerts mitochondrioprotective functions and interferes with the intra-S-phase DNA damage checkpoint. *Apoptosis: an international journal on programmed cell death* **14**, 182–190 (2009).
26. Rakhit, R. D. *et al.* Nitric oxide-induced cardioprotection in cultured rat ventricular myocytes. *American Journal of Physiol.-Heart and Circul. Physiol.* **278**, H1211–H1217 (2000).
27. Chen, I.-J. & Foloppe, N. Drug-like bioactive structures and conformational coverage with the LigPrep/ConfGen suite: comparison to programs MOE and catalyst. *J. Chem. Inform. and Model.* **50**, 822–839 (2010).
28. Halgren, T. A. *et al.* Glide: a new approach for rapid, accurate docking and scoring. 2. Enrichment factors in database screening. *J. Med. Chem.* **47**, 1750–1759 (2004).

Acknowledgements

This study was supported by a grant from a key laboratory program of the Education Commission of Shanghai Municipality (No. ZDSYS14005), National Natural Science Foundation of China (No. 81330080). National Major Scientific and Technology Special Project (No. 2012ZX09103101i-064, 2012ZX09501001-001-003).

Author Contributions

Y.W. and Y.C. contributed to the study concept and design. X.G. supervised the chemical part and Y.Z.Z. is the PI for the project. Q.Z. has provided material for the experiments. The manuscript was written through contributions of all authors. All authors have given approval to the final version of the manuscript.

Additional Information

Supplementary information accompanies this paper at <http://www.nature.com/srep>

Competing financial interests: The authors declare no competing financial interests.

How to cite this article: Wang, Y. *et al.* The discovery of a novel inhibitor of apoptotic protease activating factor-1 (Apaf-1) for ischemic heart: synthesis, activity and target identification. *Sci. Rep.* **6**, 29820; doi: 10.1038/srep29820 (2016).



This work is licensed under a Creative Commons Attribution 4.0 International License. The images or other third party material in this article are included in the article's Creative Commons license, unless indicated otherwise in the credit line; if the material is not included under the Creative Commons license, users will need to obtain permission from the license holder to reproduce the material. To view a copy of this license, visit <http://creativecommons.org/licenses/by/4.0/>